Available online at www.sciencedirect.com

SCIENCE DIRECT®

Journal of Molecular Catalysis A: Chemical 203 (2003) 37–51

JOURNAL OF MOLECULAR CATALYSIS A: CHEMICAL

www.elsevier.com/locate/molcata

Interactions of cobalt tetrasulfophthalocyanine with alkyl xanthogenates: evidence for hydrophobic effects in the Merox process

Eduard M. Tyapochkin, Evguenii I. Kozliak*

Department of Chemistry, University of North Dakota, Grand Forks, ND 58202, USA

Received 28 February 2003; received in revised form 7 April 2003; accepted 7 April 2003

Abstract

Anaerobic complexation of cobalt tetrasulfophthalocyanine (CoTSPc) with alkyl xanthogenates [ROC(S)S$^-$] has been studied by UV-Vis spectroscopy in aqueous and *N*,*N*-dimethyl formamide (DMF) solutions. In aqueous solutions, lag periods are observed in the kinetic curves for all tested xanthogenates before the axial complex is formed. The duration of this lag period decreases with elongation of the ligand's alkyl chain, thus indicating initial xanthogenate outer-sphere binding to CoTSPc. Rates of inner-sphere complexation, conversely, increase dramatically when using "longer" alkyl xanthogenates. CoTSPc–xanthogenate binding constants nearly double upon every increase of the ligand's alkyl chain by two CH_2 groups, from ethyl to *n*-octyl xanthogenate. In the aerobic Merox process (auto-oxidation of alkyl xanthogenates in the presence of CoTSPc in aqueous solutions), the rate also incrementally increases upon elongation of the substrate's alkyl chain by two CH_2 groups. The magnitude of this effect is similar to that observed for the CoTSPc–xanthogenate binding constants. In DMF, where hydrophobic interactions are not a factor, the alkyl xanthogenates display comparable kinetic and binding constants. Since the pK_a values of alkyl xanthogenic acids are similar (2.5 ± 0.1), the observed effects may be ascribed to hydrophobic interactions rather than electron donation.

Keywords: Cobalt tetrasulfophthalocyanine; Merox process; Thiol auto-oxidation; Hydrophobic interactions; Alkyl xanthogenates

1. Introduction

Auto-oxidation of basic thiolates catalyzed by cobalt phthalocyanines, e.g. cobalt tetrasulfophthalocyanine (CoTSPc, Fig. 1), is one of the primary methods used for the deodoration of petroleum products (Merox process) [1]

$$2H_2O + 4RS^- + O_2 \overset{\text{CoTSPc}}{\rightarrow} 2RSSR + 4OH^- \qquad (1)$$

A similar process has been used for controlled partial oxidation of low basicity thiolates and thioacid salts to the corresponding disulfides [2–6].

A general mechanism for reaction (1) has been suggested and successfully tested (Scheme 1) [1,7–14]. As proposed, the thiolate initially forms a binary complex with CoTSPc. This binary complex then reacts with oxygen to form a highly unstable ternary thiolate–CoTSPc–O_2 complex. Decomposition of this ternary complex leads to product formation.

Although the general reaction mechanism has been established, many fine details remain to be elucidated. For example, the role of CoTSPc association

* Corresponding author. Tel.: +1-701-777-2145; fax: +1-701-777-2331.
E-mail address: ekozliak@chem.und.edu (E.I. Kozliak).

1381-1169/03/$ – see front matter © 2003 Elsevier Science B.V. All rights reserved.
doi:10.1016/S1381-1169(03)00390-X

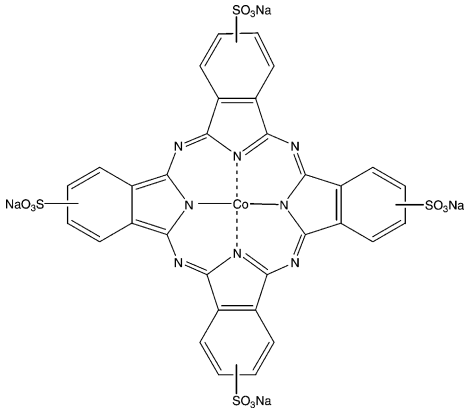

Fig. 1. Structure of Co^{II} tetrasulfophthalocyanine (CoTSPc).

in aqueous solutions in the Merox process remains unclear [8,11,14]. Also, evidence has been accumulated that suggests two, rather than one, thiolate molecules are incorporated in the ternary complex [10,15–18], which implies an outer-sphere binding of either oxygen or one of the thiolates.

Our previous studies of 1:1 CoTSPc–thiolate binary complexes conducted in aqueous media at pH 10 under anaerobic conditions showed that the oxidation state of cobalt lies between +1 and +2 (Scheme 2) [19].

Electron-donating basic thiolates bind strongly to CoTSPc, and appear to stabilize the complex due to a partial Co^{II}–Co^{I} reduction [19]. Consequently, the rate of reaction (1) increases along with the increase in substrate basicity. However, basicity does not appear to be the only major factor influencing thiolate binding to CoTSPc and reactivity in reaction (1). Both the rate of reaction (1) and the binding constant, K_{RS^-} (Scheme 2), are greater for aromatic thiolates than for aliphatic thiolates of similar basicity [19]. This may be explained by π-stacking between the conjugated aromatic systems of the thiolate and phthalocyanine ligand; ^{1}H NMR evidence for such π-stacking has been obtained [20].

In the case of aliphatic thiolates, the rate of reaction (1) has been shown to increase with the elongation of their alkyl chains [21]. Similar to π-stacking,

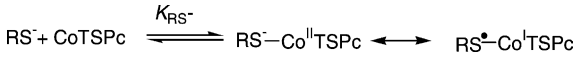

Scheme 2. Partial reduction of Co^{II}TSPc in aqueous media upon thiolate binding.

this may indicate hydrophobic interactions between the aromatic system of CoTSPc and the thiolate's alkyl group [17,22]. Unfortunately, electron donation provided by the alkyl group, R, also tends to increase upon the increase in its size, due to inductive effects. Because of the similarity in chemical structures, thiolate basicity may serve as a quantitative measure of electronic effects. Basicity of aliphatic thiolates, RS^-, gradually increases with the increase in the size of the alkyl group [23]. Thus, observed trends in the kinetics of reaction (1) may be alternatively explained by the electron donation of CH_2 groups [21]. Separation of basicity and electronic factors for regular aliphatic thiolates may not be feasible.

In the present study, we used alkyl xanthogenates instead of alkyl thiolates. The goal was to separate the influence of hydrophobic effects on the rate of reaction (1) from the electronic effects, i.e. substrate basicity. Xanthogenates are organic compounds with the following common formula: $ROC(S)S^-M^+$ (M = Na, K). The reported pK_a values of alkyl xanthogenic acids exhibit only very slight variation upon change in the number of CH_2 groups in their alkyl chains (i.e. in the second digit after the decimal point) [24]. This makes xanthogenates a suitable model system for studying the role of thiolate–CoTSPc hydrophobic interactions in reaction (1). C_2–C_8 alkyl xanthogenates were used in this study to avoid micellar effects exhibited only by larger similar ligands (as determined by viscosity measurements, not shown).

CoTSPc association will not be discussed in this paper: our previous studies have shown that dimers of CoTSPc in aqueous solutions exhibit a 1:1 stoichiometry in thiolate binding [19]. Whether or not the product was a dimer, an aggregate in an uncertain extent of polymerization, or a monomer, the same stoichiometry was observed. Therefore, regardless of the degree

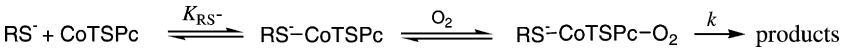

Scheme 1. Mechanism and intermediates of reaction (1).

of association, each CoTSPc molecule appears to act as an independent unit in thiolate binding.

2. Experimental

2.1. Materials

CoTSPc was provided by Dr. T.P.M. Beelen (Eindhoven Technology University, The Netherlands). Sodium and potassium salts of *n*-butyl, *n*-hexyl, and *n*-octyl xanthogenates were synthesized using a previously published procedure [25]. The corresponding alcohols were dissolved in dry diethyl ether, along with stoichiometric amounts of NaOH (KOH) followed by the addition of carbon disulfide. The resulting precipitate was recovered and purified by dissolving in acetone, filtering the solution, and then precipitating the product by slow addition of benzene. A second purification was conducted similarly, using petroleum ether instead of benzene as the precipitating agent. The resulting powder was dried to a constant weight under vacuum in a desiccator containing KOH pellets (the products were highly hygroscopic). The removal of water was monitored by recording the IR spectra: the OH stretching frequency peak at 3500 cm^{-1} ultimately disappeared upon drying (except for octyl xanthogenate, see below). Product yields were in the range of 70–80%. The potassium salt of *O*-ethylxanthic acid (EtOC(S)SK) was purchased from Aldrich as a pure, reagent grade chemical. It was purified using the same procedure as described above. Elemental analyses (conducted by Atlantic Microlab, Norcross, GA), UV-Vis, IR, ^{13}C NMR, and ^{1}H NMR (500 MHz) were used to evaluate the purity of the products. Branched isomers were the only detectable impurities, and were present in amounts not exceeding 2%. Anal. Calc. for ethyl xanthogenate [$CH_3CH_2OC(S)SK$]: C, 22.52; H, 3.40; S, 39.91; O, 10.03. Found: C, 22.58; H, 3.13; S, 40.11; O, 10.07%. For butyl xanthogenate [$CH_3(CH_2)_3OC(S)SK$]: C, 32.01; H, 4.82; S, 34.09; O, 8.58. Found: C, 32.03; H, 4.86; S, 34.12; O, 8.76%. For hexyl xanthogenate [$CH_3(CH_2)_5OC(S)SNa$]: C, 42.01; H, 6.52; S, 32.00; O, 8.06. Found: C, 41.83; H, 6.49; S, 31.77; O, 8.09%. For octyl xanthogenate [$CH_3(CH_2)_7OC(S)SNa$]: C, 47.34; H, 7.50; S, 28.07; O, 7.00. Found: C, 46.42; H, 7.49; S, 27.80; O, 8.31%. Poor elemental analysis for *n*-octyl xanthogenate was due to the presence of water (1.9–2%; detected by IR spectroscopy) that could not be removed by conventional techniques, such as drying in a desiccator with KOH pellets or under vacuum. Stoichiometrically, this percentage of H_2O corresponds to a 4:1 xanthogenate–water ratio. Taking this into account, the elemental percentage to be found in *n*-octyl xanthogenate samples becomes as follows: C, 46.42; H, 7.57; S, 27.54; O, 8.59. This corroborates with the experimentally observed values. Purified alkyl xanthogenates were stored in a desiccator with $CaCl_2$ granules. Fresh xanthogenate solutions were prepared daily.

N,*N*-dimethyl formamide (DMF) was dried with KOH, and then distilled under vacuum. The first fraction of the distillate (one-third) was discarded to remove amines. Custom-made cells for binding and kinetic studies under anaerobic conditions [15] were manufactured using Starna blanks.

2.2. Methods

The pK_a values of the conjugate acids of alkyl xanthogenates were determined by acid titration. The alkyl xanthogenate concentration was 5.0×10^{-5} M. The study was conducted in aqueous solutions with the ionic strength adjusted to 0.60 M by addition of sodium chloride at $20.0 \pm 0.1\,^{\circ}C$. Titration was done using an HCl titrant and a micropipette. Absorption peaks at 206 nm were monitored using a Shimadzu UV-2501PC spectrophotometer; only the protonated xanthogenates exhibited light absorption at this wavelength.

Spectra of the xanthogenate–CoTSPc complexes were recorded on a Shimadzu UV-2501PC spectrophotometer after mixing the degassed reagent solutions under anaerobic conditions (10^{-2} Torr vacuum). Degassing was conducted by repeating the freezing–thawing cycle three times, while applying vacuum to frozen solutions. The achievement of equilibrium was assessed by recording no further detectable change in absorbance at 626 and 665 nm for aqueous solutions and DMF, respectively, over a period of 24 h. The same wavelengths were used for monitoring the Co^{II}TSPc absorption peaks in kinetic studies. All kinetic and binding studies were performed at $20.0 \pm 0.1\,^{\circ}C$. Binding and kinetic studies in aqueous solutions were conducted in 0.15 M borate buffer (pH 10.4)

at a constant ionic strength adjusted to 0.60 M using sodium perchlorate. Sodium chloride and potassium chloride were used in selected experiments instead of sodium perchlorate, and the variation of salts did not cause any changes in the measured thermodynamic and kinetic parameters. Studies were conducted using a CoTSPc concentration of 1.0×10^{-5} M, unless otherwise indicated; sodium xanthogenate concentrations were always at least one order of magnitude larger, in the range of 1.0×10^{-4} to 1.0×10^{-1} M. ^{1}H NMR and ^{13}C NMR spectra were recorded on a Bruker Avance 500 spectrometer at 500 MHz using TMS as an internal reference. IR spectra were obtained using an ATI Mattson Genesis Series^{TM} FTIR spectrometer.

Reaction (1) kinetic experiments were conducted at 25 °C using an Instech dissolved oxygen-measuring system with a Clark electrode [19,22,26] in 0.15 M borate buffer (pH 10.4) at constant ionic strength adjusted to 0.60 M using sodium perchlorate. The concentrations of CoTSPc and oxygen were 1.0×10^{-5} and $(2.0 \pm 0.1) \times 10^{-4}$ M, respectively. Oxygen concentrations were adjusted by the time-controlled saturation of the xanthogenate solutions with nitrogen. Sodium xanthogenate concentrations were in the range of 1.0×10^{-3} to 1.0×10^{-1} M. Auto-oxidation rates of xanthogenates were measured with and without CoTSPc, and the rate of reaction (1) was calculated by subtracting the rate of the non-catalyzed reaction from that in the presence of CoTSPc. Pseudo-first-order rate constants (k_{Merox}) were calculated as the slopes of the corresponding linear plots of the auto-oxidation rate versus alkyl xanthogenate concentration.

Statistical treatment of the data was performed using standard methods [27]. For parameters calculated from the double-reciprocal plots, experimental errors (standard deviations) were determined using a linear regression statistical analysis (Origin software). In all other cases, the experimental errors were calculated as standard errors.

3. Results and discussion

3.1. pK_a values of alkyl xanthogenic acids

The pK_a values for the conjugate acids of four different xanthogenates were determined from the corresponding acid titration curves by two methods.

Table 1
pK_a values of the conjugate acids of alkyl xanthogenates in aqueous solutions containing 0.60 M NaCl

Xanthogenate	pK_a
Ethyl xanthogenate	2.5 ± 0.1
n-Butyl xanthogenate	2.4 ± 0.1
n-Hexyl xanthogenate	2.5 ± 0.1
n-Octyl xanthogenate	2.5 ± 0.1

In the first method, the pK_a was calculated as the pH value in the middle of the corresponding titration curve (Fig. 2A). Then, the obtained values were verified by a second method by which we used a double-reciprocal plot that yielded the value of K_a as a negative *x*-intercept (Fig. 2B). The two methods produced the same values (listed in Table 1) within the margin of experimental error. The data show a good correlation with the previously reported pK_a values obtained in DMF–water solutions [24]. The most important information gained from this study is that the pK_a values of the xanthogenates used are virtually the same, regardless of alkyl chain length. Thus, if any significant changes in CoTSPc–xanthogenate binding were to be observed upon elongation of the ligand alkyl group, they could not be ascribed to variations in ligand basicity.

All of the further studies were conducted at pH 10.4. At this pH, the only detectable form of any of the alkyl xanthogenates used is the deprotonated anion.

3.2. Kinetic studies

Spectral changes occurring upon the addition of alkyl xanthogenates to the aqueous solutions of Co^{II}TSPc under anaerobic conditions are shown in Fig. 3. The intensity of the phthalocyanine Q-band at 626 nm decreases with concomitant appearance of two low-intensity bands at 650 and 450 nm. Based on the information obtained previously, these spectral changes are due to Co^{II}TSPc complexation with alkyl xanthogenates followed by an incomplete Co^{II}–Co^{I} reduction, which manifests itself as a band at 450 nm [17,19,28,29]. However, the observed kinetic curves for all the xanthogenates tested are rather unusual (Fig. 4): they do not exhibit an exponential decline of absorbance as would be expected for a simple one-step reaction.

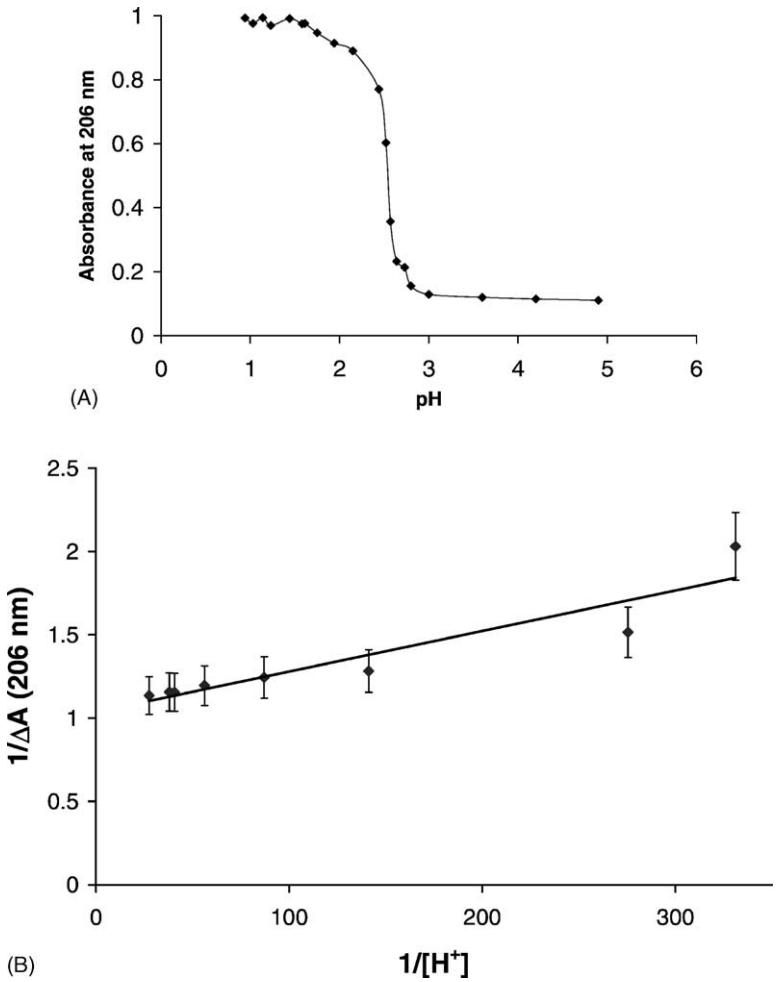

Fig. 2. (A) Changes in the ethyl xanthogenate absorbance at 206 nm upon acid titration. The concentration of ethyl xanthogenate (potassium salt) is 5.0×10^{-5} M. (B) A double-reciprocal plot based on the data of Fig. 2A. ΔA is the difference between the absorption at 206 nm of the non-protonated form of ethyl xanthogenate and its absorption at a given concentration of H^+.

The observed kinetic curves can be divided into three steps. The rates for all three steps are first-order in CoTSPc (1.0×10^{-6} to 1.0×10^{-4} M) for any xanthogenate (not shown). The first step is a lag period where the 626 nm Co^{II}TSPc Q-band and the entire spectrum slightly change over time (Fig. 3, Step 1). The lag period is labeled "Step 1" on the kinetic curves shown in Fig. 4. Discussion of the apparent chemical nature of this step is done in Section 3.3.

After the lag period, the absorption at 626 nm drops relatively fast. This "fast" step (taking a few minutes) is labeled "Step 2" on the kinetic curves shown in Fig. 4. As mentioned previously, this decrease in absorption should be attributed to inner-sphere xanthogenate complexation to the cobalt atom of Co^{II}TSPc, followed by a partial Co^{II}–Co^{I} reduction.

After the fast step, the reaction rate decreases dramatically. During this third step (taking 2–3 days), absorption at 626 nm does not change significantly, but an increase in absorption at 450 nm occurs (Fig. 3). Thus, Step 3 of the observed kinetic curves appears to correspond to the completion of the slow Co^{II}–Co^{I} reduction inside the complex.

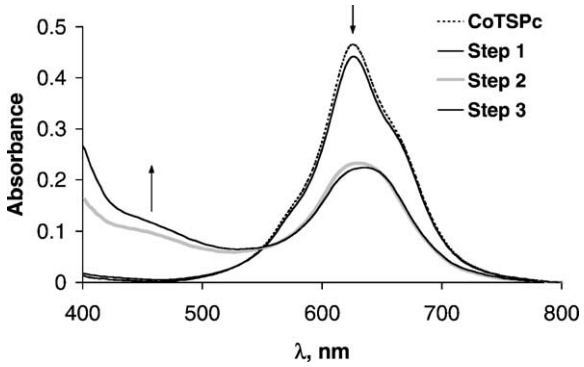

Fig. 3. UV-Vis spectra of 1.0×10^{-5} M CoTSPc in the presence of 2.5×10^{-2} M octyl xanthogenate (0.15 M borate buffer, pH 10.4, ionic strength 0.60 M) recorded under anaerobic conditions after the completion of the corresponding kinetic steps (see Fig. 4).

3.3. Mechanistic studies: ruling out dissociative mechanisms

Based on literature data, the lack of change in the UV-Vis spectrum (Fig. 3, see CoTSPc and Step 1 spectra) indicates that there is no inner-sphere complexation between the alkyl xanthogenates and Co^{II}TSPc during the lag period. Otherwise, significant changes in the Q-band absorption pattern (600–700 nm) would be observed [19,30–34].

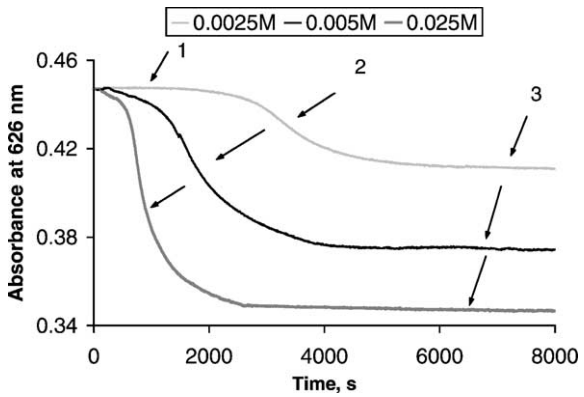

Fig. 4. Typical kinetic curves observed for the CoTSPc–octyl xanthogenate complexation in aqueous media. The 626 nm CoTSPc absorbance was monitored under anaerobic conditions at a CoTSPc concentration of 1.0×10^{-5} M (0.15 M borate buffer, pH 10.4, ionic strength 0.60 M). The ligand concentration is shown in the legend. Step 1: lag period; Step 2: "fast" step; Step 3: final kinetics.

Co^{II}TSPc exists in aqueous solutions as an aqua-complex [35–38]. Therefore, either dissociative or associative mechanisms could account for the observed lag periods. For the former, the dissociation of a water ligand from Co^{II} could be rate-limiting, thus resulting in a lag period because the intermediate, consisting of a five-coordinate Co^{II} center, would be indistinguishable from the original aqua-complex of Co^{II}TSPc (Scheme 3). Such a dissociative mechanism is unlikely because the axial water molecules of CoTSPc are known to be very labile [38].

Moreover, this hypothetic mechanism contradicts the observed dependence of the lag period duration on the concentration of the reagents. The lag period becomes shorter with the increase in concentration of Co^{II}TSPc (1.0×10^{-6} to 1.0×10^{-4} M). This would be expected for the dissociative mechanism (as for any of the alternative mechanisms discussed below). However, the duration of the lag period also decreases when the alkyl xanthogenate concentration increases (Fig. 4). This is not consistent with the simple dissociative mechanism.

A second possible dissociative mechanism (reductive dissociation) is more plausible because it would even be valid for a relatively weak attachment of water to Co^{II}TSPc (Scheme 4). The lag period for this type of mechanism would arise from autocatalysis. Once sizable amounts of the reduced species are formed, the chain reaction would start and, as a result, terminate the lag period.

This reductive dissociation mechanism would account for the observed dependence of the duration of the lag period on the alkyl xanthogenate concentration and the length of the alkyl chain (Figs. 4 and 5). As shown below under Section 3.7, the fraction of the reduced cobalt increases along with the increase in any

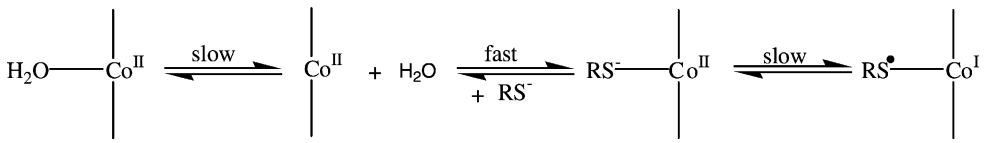

Scheme 3. A hypothetic dissociative mechanism.

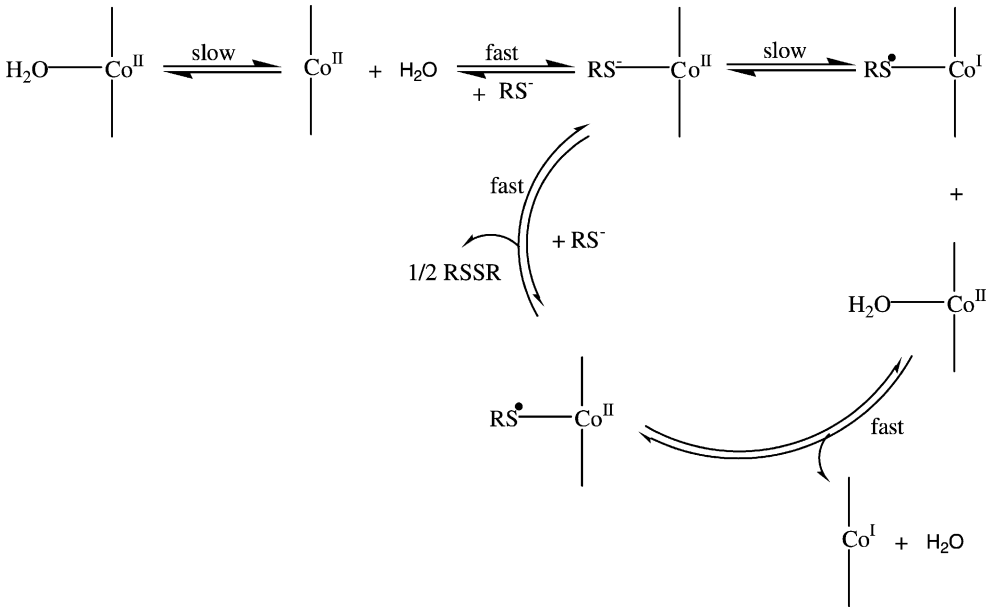

Scheme 4. A hypothetic reductive dissociative mechanism with autocatalysis.

of these two parameters. However, this mechanism was not confirmed in a direct test. In this experiment, 1.0×10^{-5} M CoTSPc was mixed with 1.0×10^{-2} M of ethyl xanthogenate under vacuum. The 626 nm absorption was monitored, and the duration of the lag periods was recorded. After a 4-day incubation, resulting in the formation of the product (an ethyl xanthogenate–CoTSPc complex with partially reduced cobalt), the entire solution was added under nitrogen (in a dry box) to a freshly mixed (under vacuum) solution of the same two reagents. The lag periods of the two experiments were then compared. Their values were 1.75×10^4 and 1.73×10^4 s, respectively, i.e. the lag periods were statistically the same as in the experiment without the prior addition of the product [$(1.7 \pm 0.1) \times 10^4$ s, Table 2]. Autocatalysis

Table 2
Duration of lag periods in the reaction of CoTSPc with alkyl xanthogenates

Xanthogenate concentration (M)	Lag period duration (s)			
	n-Octyl xanthogenate	*n*-Hexyl xanthogenate	*n*-Butyl xanthogenate	Ethyl xanthogenate
0.10	$(9.0 \pm 0.5) \times 10^1$	$(8.0 \pm 0.3) \times 10^2$	$(2.2 \pm 0.1) \times 10^3$	$(3.8 \pm 0.2) \times 10^3$
0.09	ND[a]	$(9.8 \pm 0.4) \times 10^2$	$(2.3 \pm 0.1) \times 10^3$	$(4.1 \pm 0.2) \times 10^3$
0.08	$(2.2 \pm 0.1) \times 10^2$	ND	ND	ND
0.07	$(2.4 \pm 0.1) \times 10^2$	$(1.3 \pm 0.1) \times 10^3$	$(2.7 \pm 0.1) \times 10^3$	$(6.1 \pm 0.3) \times 10^3$
0.05	$(2.8 \pm 0.1) \times 10^2$	$(2.0 \pm 0.1) \times 10^3$	$(2.9 \pm 0.1) \times 10^3$	$(6.3 \pm 0.3) \times 10^3$
0.035	ND	$(2.5 \pm 0.1) \times 10^3$	$(5.0 \pm 0.2) \times 10^3$	$(9.5 \pm 0.5) \times 10^3$
0.025	$(8.1 \pm 0.3) \times 10^2$	$(3.1 \pm 0.1) \times 10^3$	$(5.3 \pm 0.2) \times 10^3$	$(9.5 \pm 0.5) \times 10^3$
0.015	ND	$(4.0 \pm 0.1) \times 10^3$	$(5.2 \pm 0.2) \times 10^3$	$(1.5 \pm 0.1) \times 10^4$
0.01	$(1.5 \pm 0.1) \times 10^3$	$(5.1 \pm 0.2) \times 10^3$	$(7.3 \pm 0.3) \times 10^3$	$(1.7 \pm 0.1) \times 10^4$
0.005	$(2.3 \pm 0.1) \times 10^3$	ND	ND	ND

The end of the lag period is defined as the time when the CoTSPc–xanthogenate complexation rate increases by at least 80% compared to the rate during the lag period. The concentration of CoTSPc is 1.0×10^{-5} M.

[a] ND: not determined.

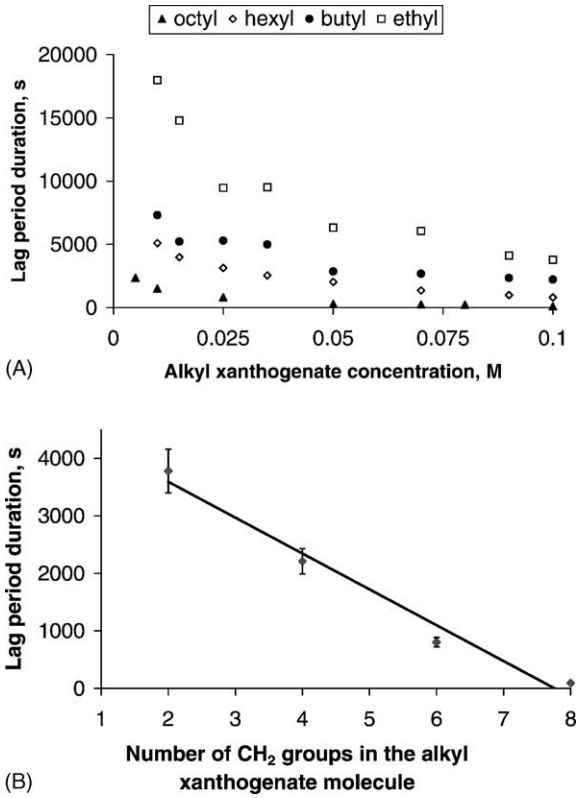

Fig. 5. (A) Duration of the lag period at varied xanthogenate concentrations. The concentration of CoTSPc is 1.0×10^{-5} M (0.15 M borate buffer, pH 10.4, ionic strength 0.60 M, under anaerobic conditions). (B) Duration of the lag period as a function of the number of CH_2 groups in the molecule of alkyl xanthogenate. The alkyl xanthogenate and CoTSPc concentrations are 0.10 M and 1.0×10^{-5} M, respectively (0.15 M borate buffer, pH 10.4, ionic strength 0.60 M, under anaerobic conditions).

would completely eliminate the lag period in the presence of the product. In addition, the kinetic curves of Step 2 yielded linear semi-logarithmic plots of absorbance versus time (not shown). This is consistent with first-order kinetics but not with autocatalysis, which would exhibit acceleration during the course of the reaction. Thus, dissociative mechanisms, with or without autocatalysis, do not appear to be valid.

3.4. Associative mechanism: evidence for outer-sphere xanthogenate–CoTSPc binding

The observed experimental data can be explained by the associative mechanism presented in Scheme 5. The xanthogenate molecule may be attached to cobalt as either the fifth or sixth ligand, depending on whether the water remains bound. This does not alter the kinetic scheme if the removal of axially-bound water is not rate-limiting.

The key element of this mechanism is the formation of an intermediate, an outer-sphere complex between the xanthogenate and CoTSPc (as shown in Step 1 of Scheme 5). The outer-sphere binding hypothesis, i.e. that the ligand's sulfur atoms are not attached to Co^{II}, explains why the spectrum of this complex is virtually indistinguishable from that of the original CoTSPc. The fast formation of a relatively stable intermediate spectroscopically indistinguishable from the initial CoTSPc would explain, in turn, the occurrence of the lag period. This mechanism supports the observed dependence of the duration of the lag period on the concentrations of both Co^{II}TSPc and the alkyl xanthogenate. Larger reagent concentrations accelerate both of the competing processes, and a fast inner-sphere complexation between the cobalt and sulfur atoms (shown as a step with K_{12} in Scheme 5) ends the lag period.

Outer-sphere binding also illustrates that the duration of the lag period significantly decreases with elongation of the xanthogenate alkyl chain (Fig. 5A and B, the values are also listed in Table 2). For instance, while switching from 0.10 M hexyl to 0.10 M octyl xanthogenate, the lag period is shorter by almost one order of magnitude; similar effects are observed for the other ligands (Table 2, Fig. 5B). Such an influence of the ligand alkyl chain size on the lag time suggests hydrophobic interactions between the xanthogenate and phthalocyanine. The molecular basis for the observed lag period may be explained as follows. Perhaps, the xanthogenate molecule must reach a certain location or conformation for the interaction between the cobalt and sulfur atoms to occur, i.e. the inner-sphere complex is thermodynamically more stable, yet its formation takes more time. Conversely, the loose outer-sphere complex forms instantly, and consequently slows down the inner-sphere coordination. Apparently, xanthogenate molecules with longer flexible alkyl chains can readjust faster and remove obstacles to the formation of the ultimate product, by means of which a thermodynamic control is exerted. The shorter the alkyl chain, the longer the time for such an adjustment. This results in the increasing role

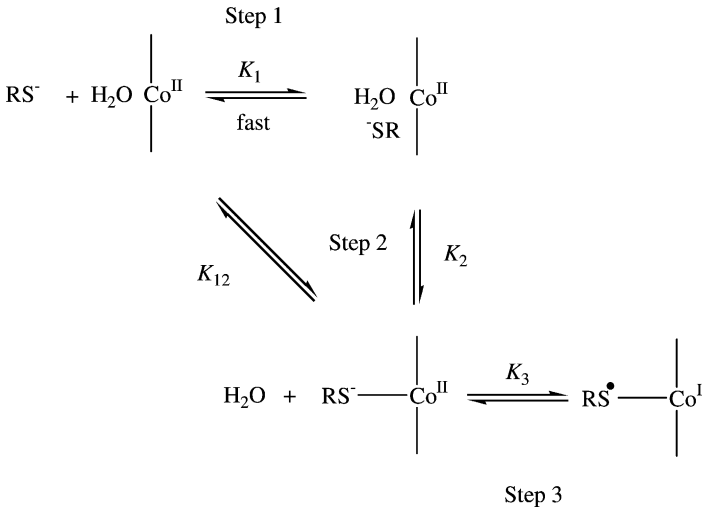

Scheme 5. CoTSPc–xanthogenate reactions in aqueous solutions.

of kinetic control when the alkyl chain decreases in size. Further evidence for this unusual "wiggling" of the xanthogenate molecules on the CoTSPc equatorial ligand was obtained in the study of the kinetics of Step 2 (Section 3.5).

Based on the data of Fig. 5A, a significant drop in the duration of the lag period occurs when the alkyl xanthogenate concentration increases above the threshold of 0.02–0.04 M; then it levels off. Therefore, the value of K_1, the outer-sphere binding constant (Scheme 5), can be estimated at 25–50 M^{-1}. This value is significantly lower than the values of K_{12} (Scheme 5) estimated from the Michaelis constants (see Section 3.5). This supports the hypothesis that the inner-sphere CoTSPc–xanthogenate binding is thermodynamically favored.

Unfortunately, our direct attempt to distinguish this outer-sphere complex from the initial CoTSPc using ^{1}H NMR (at 500 MHz) failed due to very poor spectral resolution of the phthalocyanine protons in deuterated aqueous solutions (note that Co^{II} is paramagnetic). Therefore, further arguments for the "hydrophobic" nature of the outer-sphere complex are based on evidence obtained in binding and kinetic studies.

Caution should be used in assigning Steps 2 and 3 of the observed kinetic curves to the corresponding equilibria of Scheme 5. These two steps overlap. Some reduction of cobalt (exhibited as a low-intensity absorption band at 450 nm) is observed in the end of Step 2 (Fig. 3, Step 2) even though it is formally assigned to Step 3 in Scheme 5. The experimentally measured binding constant, K_{RS^-}, appears to be a product of constants K_{12} and K_3 (or $K_1K_2K_3$) shown in Scheme 5.

3.5. Derivation and application of the kinetic equation

In Fig. 6A, the rate of the "fast" step is plotted versus the ligand concentration. Michaelis-type plots have been observed for all the xanthogenates used in this study. This observation corroborates with Scheme 5 because Michaelis kinetics implies substrate binding followed by its subsequent conversion. The experimental results may be presented as a Michaelis–Menten kinetic equation:

$$v = \frac{k[\text{CoTSPc}]_{\text{total}}[RS^-]}{K_M + [RS^-]} \quad (2)$$

where v is the observed reaction rate, i.e. the rate of the inner-sphere CoTSPc–xanthogenate complexation with partial Co^{II} reduction, K_M is the Michaelis constant, and k is the turnover number.

Standard application of a quasi-equilibrium approximation to Scheme 5 [39] (assuming k_3 to be the rate constant for the forward reaction of Co^{II} reduction) results in the following expressions for the constants

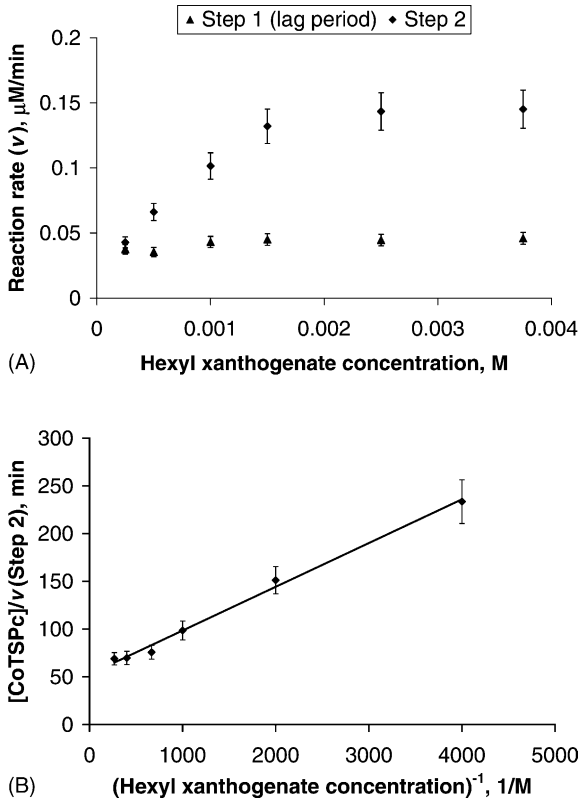

Fig. 6. (A) *n*-Hexyl xanthogenate–CoTSPc complexation reaction rates plotted at varied hexyl xanthogenate concentrations: Step 1 (lag period) and Step 2 ("fast" step; see Figs. 3 and 4). The concentration of CoTSPc is 1.0×10^{-5} M (0.15 M borate buffer, pH 10.4, ionic strength 0.60 M, under anaerobic conditions). (B) A double-reciprocal plot based on the data from Fig. 6A for Step 2 ("fast" step in the kinetics).

of the Michaelis–Menten equation:

$$k = \frac{k_3(K_1K_2 + K_{12})}{K_1 + K_1K_2 + K_{12}} \quad (3)$$

$$K_M = \frac{1}{K_1 + K_1K_2 + K_{12}} \quad (4)$$

Taking into account that K_1 is smaller than K_{12} as a result of the thermodynamic control (the inner-sphere binding is stronger than the outer-sphere binding) and that $K_1K_2 = K_{12}$ based on the principle of detailed balance (Scheme 5), these equations simplify to

$$k = k_3, \quad \text{and} \quad K_M = \frac{1}{2K_{12}} \quad (5)$$

Both the reciprocal Michaelis constant, $1/K_M$, and turnover number, k, have been determined from double-reciprocal plots like that shown in Fig. 6B using the *x*- and *y*-intercepts, respectively. Their values for the four alkyl xanthogenates tested are listed in Table 3. Examination of these values shows that the CoTSPc–xanthogenate complexation rate increases significantly with elongation of the xanthogenate alkyl chain, and most of this effect is due to the decrease in the value of K_M (Table 3 shows the corresponding increase of $1/K_M$). A significant, gradual increase in the reciprocal Michaelis constants from ethyl to octyl xanthogenate indicates hydrophobic effects in thiolate binding (Scheme 5, Steps 1 and 2). This suggestion has been confirmed by conducting binding studies (see Sections 3.6 and 3.7).

It is noteworthy that the acceleration of Step 2 observed for large-size alkyl xanthogenates (Table 3) is accompanied by shortening of the corresponding lag period (Table 2). This observation supports the proposed equilibria for Steps 1 and 2 in Scheme 5 because it implies that the inner-sphere complex formation is preceded by a competing outer-sphere complexation.

3.6. Binding constant (K_{RS^-}) determination

CoTSPc–xanthogenate binding constants, corresponding to the combination of Steps 1–3 in Scheme 5, have been determined from the UV-Vis spectra of CoTSPc with varied amounts of alkyl

Table 3
Kinetic and equilibrium constants for the 1:1 reaction of CoTSPc with alkyl xanthogenates (Schemes 3 and 4)

Xanthogenate	$1/K_M$ (M^{-1})	k (min^{-1})	K_{RS^-} (M^{-1})
Ethyl xanthogenate	$(1.4 \pm 0.6) \times 10^2$	$(0.9 \pm 0.3) \times 10^{-2}$	$(2.6 \pm 0.4) \times 10^2$
n-Butyl xanthogenate	$(3.5 \pm 0.5) \times 10^2$	$(1.2 \pm 0.2) \times 10^{-2}$	$(7.4 \pm 0.3) \times 10^2$
n-Hexyl xanthogenate	$(1.0 \pm 0.2) \times 10^3$	$(1.9 \pm 0.3) \times 10^{-2}$	$(1.3 \pm 0.1) \times 10^3$
n-Octyl xanthogenate	$(2.0 \pm 0.3) \times 10^3$	$(2.4 \pm 0.4) \times 10^{-2}$	$(2.9 \pm 0.2) \times 10^3$

Experiments have been conducted under anaerobic conditions in 0.15 M borate buffer, pH 10.4, ionic strength 0.60 M.

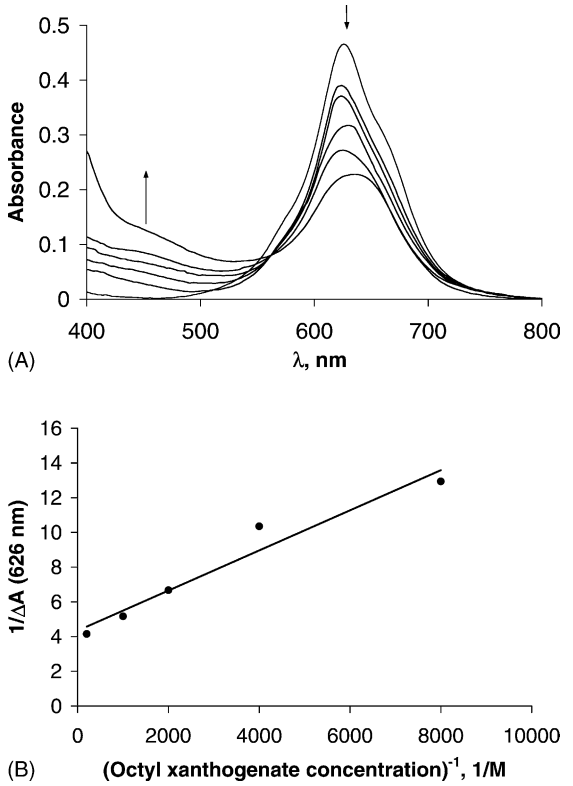

Fig. 7. (A) UV-Vis spectra of 1.0×10^{-5} M CoTSPc with increasing *n*-octyl xanthogenate concentrations at equilibrium (0.15 M borate buffer, pH 10.4, ionic strength 0.60 M, under anaerobic conditions). Concentrations of *n*-octyl xanthogenate are 0 (fine line), 1.25×10^{-4}, 2.5×10^{-4}, 1.0×10^{-3}, 5.0×10^{-3} M (dark lines). The arrows indicate the absorption changes upon increase in octyl xanthogenate concentration. (B) A double-reciprocal plot based on the data from Fig. 7A. ΔA is the difference between the absorption at 626 nm of the initial CoTSPc and that at a given concentration of *n*-octyl xanthogenate.

xanthogenates (shown for octyl xanthogenate in Fig. 7A). It can be seen from Fig. 7A that the initial CoTSPc spectrum does not pass through the isosbestic point. This observation indicates that there is more than one form present in the solution during the CoTSPc–xanthogenate complexation, thus corroborating with our hypothesis on the formation of an outer-sphere complex (Step 1, Scheme 5). In Fig. 7B, the change in the CoTSPc absorption at 626 nm upon the addition of octyl xanthogenate is plotted as a double-reciprocal plot versus the ligand concentration. Similar straight lines have been obtained for all four substrates tested (not shown), indicating the 1:1 CoTSPc–xanthogenate stoichiometry.

K_{RS^-} values were determined from the *x*-intercepts of the double-reciprocal plots for the corresponding alkyl xanthogenates (a detailed derivation for the calculation of binding constants was presented in an earlier paper [19]). K_{RS^-} values are listed in the last column of Table 3; these constants exhibit the same trends and values as the reciprocal values of the corresponding Michaelis constants (Table 3, Column 2). The binding constants are similar to but somewhat larger than the corresponding values of $1/K_M$. This is expected because, based on their derivation from Scheme 5, K_{RS^-} and $1/K_M$ are different by the value of K_3 ($K_3/K_M = 2K_3K_{12} = K_{RS^-}$). In addition, the quasi-equilibrium approach is approximate, so the Michaelis constants may depend on some kinetic parameters of Scheme 5 as well [39].

3.7. Hydrophobic effects in CoTSPc–xanthogenate binding

As shown in the last column of Table 3, the values of equilibrium constants gradually increase from ethyl to octyl xanthogenate. K_{RS^-} almost doubles each time the ligand's alkyl chain is increased in size by two CH_2 groups. Since the xanthogenate basicity is not affected by the length of its alkyl chain (see Table 1), this appears to indicate that hydrophobic interactions are responsible for the change in K_{RS^-}. Apparently, a longer alkyl chain provides greater xanthogenate affinity to the CoTSPc aromatic system not only within the outer-sphere complex, but also within the inner-sphere complex. Thus, the phthalocyanine and ligand may be connected not only by cobalt and sulfur, but also by their non-polar parts. To validate this hypothesis, we have plotted $\log K_{RS^-}$ versus $\log P_{ROH}$, where P_{ROH} is the *n*-octanol–water partition coefficient of a corresponding alcohol (serving as a measure of substrate hydrophobicity [40]; Fig. 8). The plot is linear, thus implying a linear correlation between free energies of binding and hydrophobic interactions. It is noteworthy that if the observed increase in CoTSPc binding were due to the electron donation of the CH_2 groups in alkyl xanthogenates, the most notable increase in K_{RS^-} would be observed for the change from ethyl to butyl xanthogenates, followed by its leveling off upon

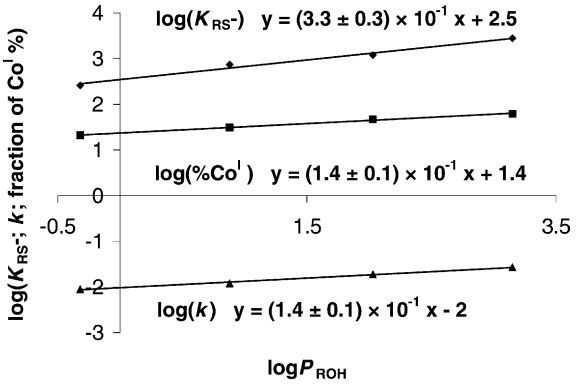

Fig. 8. A double-logarithmic plot of the CoTSPc–xanthogenate kinetic and binding constants (k and K_{RS^-}, respectively), and the fraction of reduced cobalt (Co^{I} (%)) vs. P_{ROH} (n-octanol–water partition coefficient for the corresponding alcohol).

further elongation of the alkyl group: this was not experimentally observed (Table 3).

Another thermodynamic parameter of the investigated system, e.g. the degree of Co^{II}–Co^{I} reduction, also depends on the length of the xanthogenate alkyl chain. Absorbance at 450 nm in the UV-Vis spectra at equilibrium (measuring the Co^{II}–Co^{I} reduction [17,19,22,28,29]) was plotted versus xanthogenate concentration in Fig. 9. This absorbance and, thus, the fraction of Co^{I} (calculated based on the absorbance of a pure reduced form at 450 nm [19]), increase

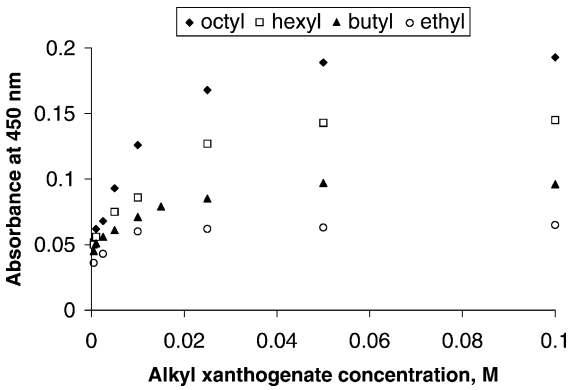

Fig. 9. The 450 nm absorbance of the CoTSPc complexes with ethyl, n-butyl, n-hexyl, and n-octyl xanthogenates at equilibrium plotted vs. the ligand concentration. The concentration of CoTSPc is 1.0×10^{-5} M (0.15 M borate buffer, pH 10.4, ionic strength 0.60 M, under anaerobic conditions).

incrementally from ethyl to octyl xanthogenate at any given concentration. This could be explained by the stronger CoTSPc binding to "longer" alkyl xanthogenates that results in shortening of the S–Co bond, thus promoting metal reduction. An alternate or complementary explanation may be based on microenvironment change. If the axial ligand is more hydrophobic, the microenvironment around the cobalt atom becomes less polar. In turn, this destabilizes the separation of charges between the cobalt and sulfur atoms in the inner-sphere complex, thus making Co^{II} reduction more favorable. In a sense, this would comprise a hidden electronic effect based on π-donation.

However, a quantitative comparison of hydrophobic effects in binding and reduction shows that the observed 3-fold increase in the reduced form fraction, while switching from ethyl to octyl xanthogenate, does not account for a 10-fold increase of K_{RS^-}. This can also be seen from the double-logarithmic plot in Fig. 8. The observed slope for the fraction of the reduced cobalt in Fig. 8 is significantly smaller than that for K_{RS^-}. Thus, the hydrophobic effects go beyond creating a less polar microenvironment for cobalt reduction.

The microenvironment effect, however, may explain a slight increase of the kinetic constant, k, observed upon the increase of the ligand hydrophobicity (Table 3). The value of this constant also increases only 2.5–3 times upon switching from ethyl to octyl xanthogenate, and the slopes of the double-logarithmic plots in Fig. 8 are similar for k and the percentage of Co^{II} reduction. Less polar environment created by the coordination of more hydrophobic ligands appears to stabilize the less charged transition state (the last reaction in Scheme 5) thus accelerating the metal reduction.

3.8. Complexation of CoTSPc with alkyl xanthogenates in DMF

To further validate our hypothesis on hydrophobic interactions between CoTSPc and alkyl xanthogenates, a series of studies similar to those done in aqueous solutions were conducted in DMF. DMF does not exhibit any hydrogen bonding; thus, hydrophobic interactions in DMF are not a factor. Therefore, no significant differences in CoTSPc–xanthogenate

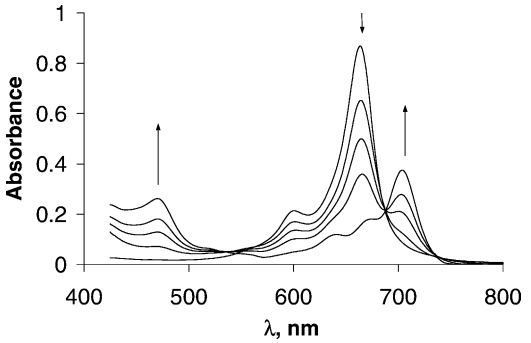

Fig. 10. CoTSPc (1.0×10^{-5} M) spectra at equilibrium upon the addition of increasing concentrations of ethyl xanthogenate in DMF (under anaerobic conditions). Concentrations of ethyl xanthogenate are 0 (fine line), 8.0×10^{-4}, 2.5×10^{-3}, 1.0×10^{-2}, and 1.0×10^{-1} M (dark lines). The arrows indicate the absorption changes with the increase in ethyl xanthogenate concentration.

kinetics and binding for the four xanthogenates should be observed in DMF solution.

CoTSPc spectra upon addition of increasing amounts of the potassium salt of ethyl xanthogenate (at equilibrium) are presented in Fig. 10. The difference in the initial spectra shown in Figs. 7A and 10 is due to the Co^{II}TSPc association that occurs in aqueous solutions but not in DMF [35,36,41]. In a previous paper, we reported a detailed kinetic and binding study on the interactions of CoTSPc with ethyl xanthogenate (potassium salt) in DMF [20]. Our goal in the present study was to determine whether the complexation strength and rate depend on the size of the alkyl chains. Therefore, we have recorded the initial kinetics, and compared the initial and equilibrium spectra for four different xanthogenates (monitoring the decrease in time of the Co^{II}TSPc absorbance peak at 665 nm). The reaction rate is first-order in both xanthogenate (1.0×10^{-3} to 5.0×10^{-2} M) and CoTSPc (1.0×10^{-6} to 1.0×10^{-4} M):

$$v = k_{DMF}[CoTSPc][RS^-] \quad (6)$$

The values of binding constants (K_{DMF}, determined as described above for aqueous solutions) and kinetic constants (k_{DMF}, calculated as the slopes of the straight lines in the plots of CoTSPc–xanthogenate complexation rate versus xanthogenate concentration) are listed in Table 4. The values of K_{DMF} and k_{DMF} for all of the tested xanthogenates are the same, within the margin of statistical errors. This indicates that in DMF, i.e. in the absence of hydrophobic interactions, both the strength and rate of the CoTSPc–xanthogenate complexation are independent of the ligand's alkyl chain size. This observation underscores the fact that in aqueous solutions the differences in kinetic and binding parameters for different alkyl xanthogenates are due to hydrophobic interactions.

Table 4
Kinetic and equilibrium constants for the 1:1 complexation reaction of CoTSPc with alkyl xanthogenates in DMF under anaerobic conditions

Xanthogenate	k_{DMF} (min^{-1})	K_{DMF} (M^{-1})
Ethyl xanthogenate	$(4.5 \pm 0.5) \times 10^{-1}$	$(7.1 \pm 0.2) \times 10^{2}$
n-Butyl xanthogenate	$(4.9 \pm 0.5) \times 10^{-1}$	$(7.5 \pm 0.3) \times 10^{2}$
n-Hexyl xanthogenate	$(3.9 \pm 0.4) \times 10^{-1}$	$(6.9 \pm 0.3) \times 10^{2}$
n-Octyl xanthogenate	$(5.1 \pm 0.6) \times 10^{-1}$	$(7.3 \pm 0.2) \times 10^{2}$

The concentration of CoTSPc is 1.0×10^{-5} M.

3.9. Hydrophobic interactions in the kinetics of the Merox process

The information presented above is only significant as long as it is applicable to the Merox process (reaction (1)). Therefore, kinetic experiments on CoTSPc–catalyzed auto-oxidation of alkyl xanthogenates have been conducted. First-order kinetics has been observed for reaction (1) on all of the three reagents (xanthogenate, CoTSPc, and O_2) within the following concentration ranges: CoTSPc (1.0×10^{-6} to 1.0×10^{-4} M), any xanthogenate tested (1.0×10^{-3} to 1.0×10^{-1} M), and oxygen (1.0×10^{-5} to 2.5×10^{-4} M) (not shown). Pseudo-first-order rate constants (k_{Merox}), calculated as slopes in the linear plots of reaction (1) rates versus the concentrations of the corresponding xanthogenates, are listed in Table 5. The rate constants increase gradually upon extension of the xanthogenate alkyl chain (Table 5).

As discussed above, the basicity of alkyl xanthogenates as a measure of electron donating factor does not show any change with elongation of the alkyl chain (Table 1). Thus, the auto-oxidation rate appears to depend only on the substrate hydrophobicity. Moreover, the double-logarithmic plot of k_{Merox} versus the hydrophobicity parameter, P_{ROH}, is linear (Fig. 11) indicating a free energy correlation. It is noteworthy

Table 5
Reaction (1) pseudo-first-order rate constants for alkyl xanthogenates, k_{Merox}, calculated as slopes of the corresponding linear plots of the auto-oxidation rate vs. alkyl xanthogenate concentration

Xanthogenate	k_{Merox} (min^{-1})
Ethyl xanthogenate	$(1.4 \pm 0.1) \times 10^{-1}$
n-Butyl xanthogenate	$(3.2 \pm 0.2) \times 10^{-1}$
n-Hexyl xanthogenate	$(6.7 \pm 0.6) \times 10^{-1}$
n-Octyl xanthogenate	2.6 ± 0.3

Experiments have been conducted at 25 °C in 0.15 M borate buffer (pH 10.4) at a constant ionic strength adjusted to 0.60 M by the addition of sodium perchlorate. The concentrations of CoTSPc and oxygen are 1.0×10^{-5} and $(2.0 \pm 0.1) \times 10^{-4}$ M, respectively.

that if the increase in pseudo-first-order rate constants (k_{Merox}) were due to the electronic donation of the CH_2 groups, it would be particularly pronounced while switching from ethyl to butyl xanthogenate, and would be greatly diminished upon further elongation of the alkyl group. However, this was not observed in the experiment (Table 5). It should also be noted that the slope of this plot (Fig. 11) is statistically the same as that obtained for the xanthogenate–CoTSPc binding constants, K_{RS^-} (Fig. 8): $(3.1 \pm 0.4) \times 10^{-1}$ and $(3.3 \pm 0.3) \times 10^{-1}$, respectively. This indicates that the increase in the rate of the Merox process is due to an increase in the xanthogenate–CoTSPc binding constant. The stronger the substrate binding, the greater the concentration of the intermediate and, thus, the faster reaction (1).

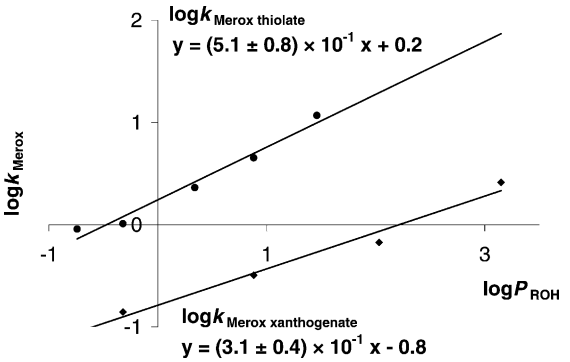

Fig. 11. A double-logarithmic plot of the Merox process rate constants for thiolates and xanthogenates, $k_{Meroxthiolate}$ and $k_{Meroxxanthogenate}$, vs. P_{ROH} (*n*-octanol–water partition coefficient for the corresponding alcohol). The data for the thiolates are taken from [21].

This observation corroborates with a trend reported earlier: the first-order rate constants of reaction (1) increase with the alkyl chain elongation in aliphatic thiolates (rather than xanthogenates) [21]. A similar double-logarithmic plot of rate constants for non-branched alkyl thiolates versus the hydrophobicity parameter also yields the straight line (Fig. 11) as was the case for xanthogenates. Therefore, the effect of the ligand's alkyl chain elongation on the reaction rate is qualitatively similar for thiolates and thioacids. A larger slope value for alkyl thiolates $(5.1 \pm 0.8) \times 10^{-1}$ (as compared to alkyl xanthogenates) apparently indicates that the CoTSPc–thiolate binding is due to a combination of hydrophobic and inductive (basicity) effects because the higher molecular weight aliphatic thiolates also have a greater basicity [23]. By contrast, electronic effects are less significant in the case of alkyl xanthogenates characterized by similar basicities (Table 1). The low basicity of alkyl xanthogenates results in their lower auto-oxidation rates as compared to alkyl thiolates of similar hydrophobicity (shown as points in two different straight lines in Fig. 11).

4. Conclusion

Even though evidence for hydrophobic interactions between the thiolate-ion and CoTSPc obtained in this study is indirect, it is based on significant and consistent trends in thermodynamic and kinetic parameters. These trends cannot be accounted for by inductive effects (i.e. ligand basicity or π-donation), are observed in aqueous media but not in DMF (i.e. are relevant to hydrophobicity), and correlate with each other (i.e. kinetic and binding constants in xanthogenate–CoTSPc complexation and Merox process kinetics for both alkyl thiolates and thioacids). Combining the results of this study with those of aromatic thiolate binding to CoTSPc [19,20], we may conclude that the outer-sphere interactions of phthalocyanines with thiolates and anions of thioacids appear to play a significant role in both the rate of the Merox process and substrate binding.

Acknowledgements

The authors thank Dr. T.P.M. Beelen, Eindhoven Technology University, The Netherlands, for

providing CoTSPc. The work was in part supported by NSF-EPSCoR, NSF Grant # OSR-9452892. The authors are immensely grateful to UND Faculty Senate and Research Committee for sponsoring the presentation of the obtained results at the Second International Symposium on Porphyrins and Phthalocyanines in Kyoto, Japan in July 2002. The authors are grateful to Dr. A.N. Vedernikov (Indiana University) for reading the manuscript and providing valuable suggestions.

References

[1] B. Basu, S. Satapathy, A.K. Bhutnagar, Catal. Rev. 35 (1993) 571.
[2] T.A. Ananieva, G.F. Titova, V.F. Borodkin, Izv. Vyssh. Uchebn. Zaved. U.S.S.R., Khim. Khim. Tekhnol. 22 (1979) 37.
[3] T.A. Ananieva, G.F. Titova, V.F. Borodkin, Izv. Vyssh. Uchebn. Zaved. U.S.S.R., Khim. Khim. Tekhnol. 25 (1982) 706.
[4] G.F. Titova, T.A. Ananieva, T.E. Kuznetsova, Izv. Vyssh. Uchebn. Zaved. U.S.S.R., Khim. Khim. Tekhnol. 24 (1981) 445.
[5] A.K. Yatsimirskii, E.I. Kozliak, A.S. Erokhin, V.E. Vigdergauz, I.V. Berezin, React. Kinet. Catal. Lett. 34 (1987) 439.
[6] V.E. Vigdergauz, A.K. Yatsimirskii, V.A. Chanturiya, E.I. Kozliak, V.V. Faydelj, A.S. Erokhin, M.V. Teplyakova, N.K. Gromova, USSR Patent 1,334,446 (1987).
[7] J. Dolinsky, D.M. Wagnerova, J. Veprek-Siska, Collect. Czech. Chem. Commun. 41 (1976) 2326.
[8] W.M. Brouwer, P. Piet, A.L. German, J. Mol. Catal. 22 (1984) 297, and references therein.
[9] M.R. Hoffmann, A.P.K. Hong, Sci. Total Environ. 64 (1987) 99.
[10] P.-S.K. Leung, E.A. Betterton, M.R. Hoffmann, J. Phys. Chem. 93 (1989) 430.
[11] P.-S.K. Leung, M.R. Hoffmann, J. Phys. Chem. 93 (1989) 434.
[12] J. van Welzen, A.M. van Herk, A.L. German, Makromol. Chem. 189 (1988) 587.
[13] A.M. van Herk, A.H.J. Tullemans, J. van Welzen, A.L. German, J. Mol. Catal. 44 (1988) 269.
[14] E.T.W.M. Schipper, J.P.A. Heuts, R.P.M. Pinckaers, P. Piet, A.L. German, J. Polym. Sci. A: Polym. Chem. 33 (1995) 1841, and references therein.
[15] E.I. Kozliak, A.S. Erokhin, A.K. Yatsimirskii, I.V. Berezin, Bull. Acad. Sci. U.S.S.R., Div. Chem. Sci. (1986) 741.
[16] E.I. Kozliak, A.S. Erokhin, A.K. Yatsimirskii, React. Kinet. Catal. Lett. 33 (1987) 113.
[17] A.K. Yatsimirskii, E.I. Kozlyak, A.S. Erokhin, Kinet. Catal. 29 (1988) 305.
[18] H. Fisher, G. Schultz-Ekloff, D. Wöhrle, Chem. Eng. Technol. 20 (1997) 624.
[19] A. Navid, E.M. Tyapochkin, Ch.J. Archer, E.I. Kozliak, J. Porphyrins Phthalocyanines 3 (1999) 654.
[20] E.M. Tyapochkin, E.I. Kozliak, J. Porphyrins Phthalocyanines 5 (2001) 405.
[21] V.A. Fomin, A.M. Mazgarov, N.N. Lebedev, J. Neftekhimiya 18 (1978) 294.
[22] E.I. Kozliak, A. Navid, Prepr. ACS Div. Fuel Chem. 42 (1997) 56.
[23] M.R. Crampton, in: S. Patai (Ed.), Chemistry of the SH Group, Plenum Press, New York, 1976, p. 397.
[24] K. Hayachi, I. Sasaki, S. Inomata, T. Yanasidani, Bull. Chem. Soc. J. 57 (1984) 3074.
[25] D.L. Vincent, C.B. Purves, Can. J. Chem. 34 (1956) 1302.
[26] E.I. Kozliak, Prepr. ACS Div. Petrol. Chem. 41 (1996) 628.
[27] A.J. Gordon, R.A. Ford, The Chemist's Companion, Wiley, New York, 1972, p. 512.
[28] M.J. Stillman, A.J. Thomson, J. Chem. Soc., Faraday Trans. II (1974) 790.
[29] P.C. Minor, M. Gouterman, A.B.P. Lever, Inorg. Chem. 24 (1985) 1894.
[30] G.V. Ouedraogo, C. More, Y. Ritchard, D. Benlian, Inorg. Chem. 20 (1981) 4387.
[31] J.A. De Bolfo, T.D. Smith, J.F. Boas, J.R. Pilbrow, J. Chem. Soc., Faraday Trans. II (1976) 481.
[32] D.J. Cookson, T.D. Smith, J.F. Boas, P.R. Hicks, J.R. Pilbrow, J. Chem. Soc., Dalton Trans. (1977) 109.
[33] M. Sekota, T. Nyokong, Polyhedron 15 (1997) 3279.
[34] J. Mack, M.J. Stillman, Inorg. Chem. 36 (1997) 413.
[35] L.C. Gruen, J. Blagrove, Aus. J. Chem. 26 (1973) 319.
[36] E.W. Abel, J. Pratt, R. Whelan, J. Chem. Soc., Dalton Trans. (1976) 509.
[37] R.D. George, A.W. Snow, J.S. Shirk, W.R. Barger, J. Porphyrins Phthalocyanines 2 (1998) 1.
[38] A.B.P. Lever, M.R. Helmstead, C.C. Leznoff, W. Liu, M. Melnik, W.A. Nevin, P. Seymour, Pure Appl. Chem. 58 (1986) 1467.
[39] A. Fersht, Enzyme Structure and Mechanism, Freeman, New York, 1984, p. 102.
[40] A. Leo, C. Hunch, D. Elkins, Chem. Rev. 71 (1971) 525.
[41] P. Day, P.A. O'Hill, M.G. Price, J. Chem. Soc. A (1968) 90.